Multiscale dynamics and robust critical scaling in a continuum current sheet model

V. M. Uritsky*
National Research Council at NASA / Goddard Space Flight Center, Greenbelt, Maryland 20770

A. J. Klimas
NASA / Goddard Space Flight Center, Greenbelt, Maryland 20770

D. Vassiliadis
Universities Space Research Association, Seabrook, Maryland

(Received 14 August 2001; published 28 March 2002; publisher error corrected 25 April 2002)

We analyze the self-organized critical behavior of a continuum running avalanche model. We demonstrate that over local interaction scales, the model behavior is affected by low-dimensional chaotic dynamics that plays the role of the primary noise source. With the help of scale-free avalanches, the uncertainty associated with chaos is distributed over a variety of intermediate scales and thus gives rise to spatiotemporal fluctuations that are characterized by power-law distribution functions. We show that globally, the continuum model displays structurally stable critical scaling that can be observed in a finite region in the control parameter space. In this region, the system exhibits a power-law critical divergence of the integrated response function over a broad range of dissipation rates. The observed behavior involves a remarkably stable spatial configuration. We explain the robust features of the model by the adjustable dynamics of its global loading-unloading cycle, which allows maintaining the long-term stationary state without affecting the intrinsic avalanche dynamics.

DOI: 10.1103/PhysRevE.65.046113 PACS number(s): 05.65.+b, 05.45.−a, 05.70.Jk

I. INTRODUCTION

The phenomenon of self-organized criticality (SOC) associated with the formation of a stable critical point in open systems with many degrees of freedom [1] has drawn considerable attention within the last decade. Nevertheless, it's explanation and primary mechanism remain controversial.

The original interpretation of the manner in which a system arrives in the SOC state implies that this process does not require tuning of any external parameters [2]. This point of view is in agreement with early studies that were focused on the critical behavior of internal relaxation events (avalanches) that were considered instantaneous with respect to the driving time scale [3–5].

A second, more recent interpretation is that the SOC state has some hidden control parameters that must be carefully tuned before the system can reach the critical state. This approach emphasizes the fact that the infinite time separation between the external driving force and the internal dynamics requires tuning the driving rate to zero. The dissipation rate also must be tuned to zero since many of the SOC models, including the prototypical sandpile model, lose the SOC state when some amount of the transported dynamical variable is annihilated [6,7]. Using a mean-field approach, it has been shown analytically [8] that in sandpile and forest-fire models of SOC, the driving rate h and the dissipation rate ε are in indeed relevant control parameters. Criticality is only obtained in the limit of vanishing h and ε, provided the ratio h/ε is infinitesimally small. It has been suggested that analogous parametric dependencies underlie the critical behavior of any SOC models with multiple absorbing states [8].

A possible compromise between these two points of view on the essence of the SOC state has been discussed recently by Kinouchi and Prado [7]. They have proposed that in some SOC systems, the critical dynamics can involve only weak dependence on variations of the control parameters around the SOC point. Such a weak dependence may provide a chance to observe signatures of a near-critical behavior that in practice is undistinguishable from ''pure'' criticality in a vast range in the parameter space.

In this paper, we demonstrate that the robust scaling behavior similar to that described in Ref. [7] can arise in a continuum avalanche system. The model was proposed by Lu [9] and later modified by Klimas *et al.* [10] to studying multiscale turbulence in the current sheet of Earth's magnetospheric tail. The dynamics of the model includes a hierarchy of turbulent effects ranging from low-dimensional chaos on the level of localized instabilities to multiscale avalanche dynamics obeying scale-free probability distributions characteristic of the SOC state. We show both analytically and numerically that although complete criticality in this system exists only at a single point where h and ε are tuned to zero in accordance with theoretical results of Ref. [8], there is a wide range of the control parameters providing clear power-law divergence of the integrated response function and, therefore, satisfying the conditions of structurally stable near-critical dynamics.

II. THE CURRENT SHEET MODEL

The first equation of the current sheet model developed by Klimas *et al.* [10] is obtained through a reduction of the resistive magnetohydrodynamic (MHD) system to a one-

*Present address: Institute of Physics, St. Petersburg State University, St. Petersburg, Russia;
Electronic address: uritsky@geo.phys.spbu.ru

dimensional limit in which the magnetic field has only an x component and all quantities vary in the orthogonal z direction only. In this limit

$$\frac{\partial B_x(z,t)}{\partial t} = \left[\frac{\partial}{\partial z} D(z,t) \frac{\partial B_x}{\partial z} \right] + S(z,t), \tag{1}$$

in which the dimensionless diffusion coefficient is given in terms of the resistivity $\eta(z,t)$ by $D(z,t) = c^2 \eta(z,t) L V_a / 4\pi$, where V_a is a measure of the Alfven velocity in the plasma and L is half of the system length (see below). Equation (1) is decoupled from the rest of the MHD system through the assumption of $S(z,t)$ as a given constant source: $S(z) = S_0 \sin(\pi z / 2L)$. The second model equation was adopted from Lu [9]. In Ref. [10], this equation describes the time evolution of the diffusion coefficient due to the formation of anomalous resistivity:

$$\partial D / \partial t = (Q(z,t) - D)/\tau,$$

$$Q(z,t) = \begin{cases} D_{\max} & |\partial B_x / \partial z| > k, \\ D_{\min} & |\partial B_x / \partial z| < \beta k, \end{cases} \tag{2}$$

where $D_{\max} \gg D_{\min}$. Here, the parameter $Q(z,t)$ introduces the effects of a current driven instability into the model; it is either in the excited state ($Q = D_{\max}$) or the quenched state ($Q = D_{\min}$). According to Eq. (2), the transition from the quenched to the excited state takes place when and wherever the field gradient exceeds a critical value k, whereas the transition back to the quiet state occurs if the gradient becomes lower than βk, where $\beta < 1$. The diffusion coefficient follows Q with the delay time τ.

The above equations were integrated numerically using a leapfrog integration scheme on a discrete grid in the spatial interval $-L \leqslant z \leqslant L$, subject to boundary conditions $\partial B_x / \partial z = 0$ at $z = \pm L$. The boundary conditions prevent flux from escaping the region through the boundaries and the source function has the effect of steadily introducing opposing magnetic flux into the current sheet. In our calculations, we used the following set of the model parameters: $D_{\min} = 0$; $D_{\max} = 5$; $L = 20$; $\tau = 1$; $\beta = 0.9$. The remaining two parameters, S_0 and k, were varied as specified below.

The system (1), (2) can be considered an idealized one-dimensional model of a magnetic field reversal in which the dynamics of the system are due to spatiotemporal magnetic field annihilation. Besides the specific field geometry, an important feature of this model is the absence of external noise. The system displays two levels of activity. On a long time scale, the dynamics consists of system-wide unloading (field annihilation) events separated by quiet loading periods. During the unloading intervals, the system exhibits spatiotemporal turbulence characterized by $1/f$-like power spectral density and power-law distribution functions of individual localized instabilities analogous to avalanches in sandpile models of SOC [10,11].

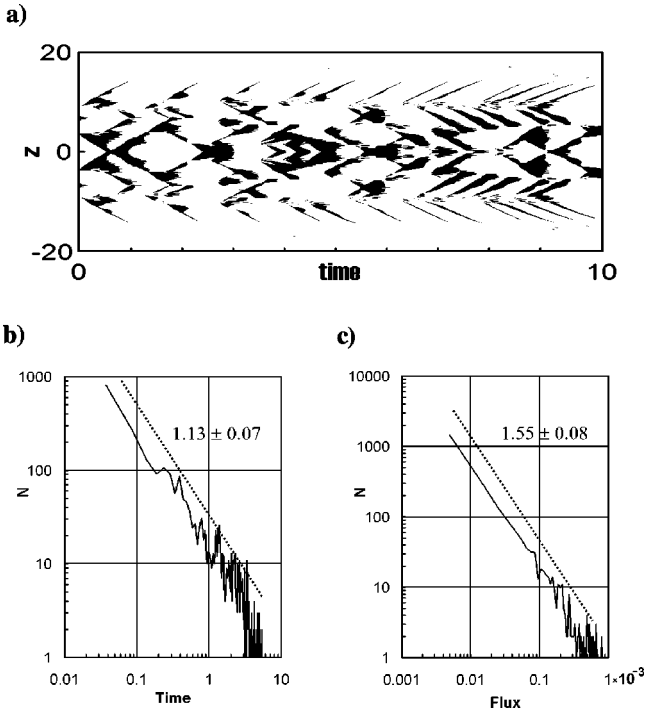

FIG. 1. (a) Example of spatiotemporal dynamics of the diffusive flux during an unloading interval ($k = 0.002$, $D_{\max} = 5$). Black areas satisfy the condition $|D(\partial B_x / \partial z)| > f$ and are treated as avalanches. (b),(c) Distributions over the lifetime and transported flux of the avalanches based on the analysis of three global unloading events with the same parameters as in the top plate. Slope values are shown with standard errors.

III. AVALANCHE DYNAMICS AND DETERMINISTIC CHAOS

To quantify the statistics of current sheet instabilities during the unloading events, we have analyzed the model dynamics on spatiotemporal plots of the diffusive flux $-D(\partial B_x / \partial z)$. Since the duration of localized excitations ($Q = D_{\max}$) is typically much shorter than the relaxation time τ of the diffusion coefficient, the spatiotemporal analysis allows the recognition of instabilities developing concurrently but independently in different regions of the current sheet. To locate the instabilities, we applied a constant threshold f. The current sheet elements with absolute value of the diffusive flux greater than f and making up a contiguous pattern on the $z-t$ plane were considered to be parts of the same relaxation process (avalanche). As an example, Fig. 1 shows the spatiotemporal dynamics and probability distributions over lifetime and total transported flux of the avalanches obtained with $f = 2.5 \times 10^{-2} k\, D_{\max}$. It can be seen that the distributions have a clear power-law form characteristic of systems at or near the SOC state. The power-law exponents obtained for lifetime and flux distributions are, respectively, 1.13 ± 0.07 and 1.55 ± 0.08. A similar behavior has been observed for the perturbation length distribution, with the power exponent 1.04 ± 0.10.

The primary mechanism of the stochastic model behavior during the unloading intervals calls for special investigation. Indeed, although the model equations do not include any

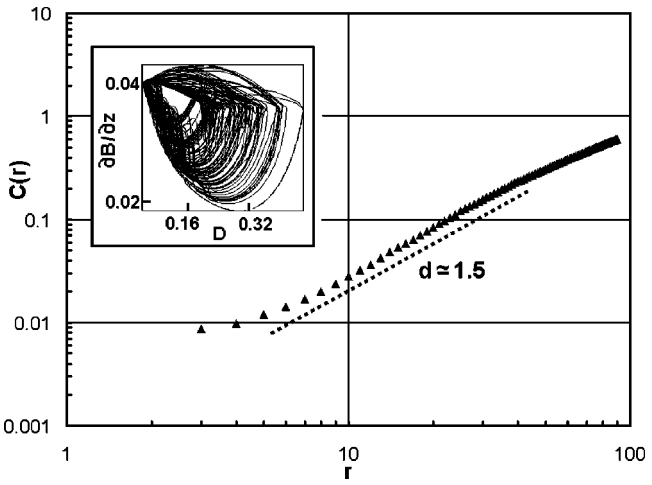

FIG. 2. The correlation integral statistics (number C of pairs of phase points separated by the distance less than r) for the Poincaré cross section in the coordinates $\partial B_x(z,t)/\partial z, \partial B_x(z,t-T)/\partial z$ representing the local grid site coupling dynamics ($D=0.16$, $T=0.05$, $n=3$, $f_{inp}=0.005$). The inset: a view of a phase portrait at the same parameter values.

explicit sources of noise, its dynamics exhibits an apparent stochastic component. We have found that, in the absence of a noise source, this randomness is produced by a deterministic chaos due to local nonlinear interactions between the current sheet elements. In order to test this effect, we have studied the dynamics of a small number n of neighboring grid sites obeying Eqs. (1), (2). The grid sites were subjected to a constant input flux f_{inp} through one of the boundaries and an open boundary condition at the opposite boundary. Such a subsystem mimics the propagation of the avalanches through a small region of the current sheet.

A numerical study has shown that in the cases $n=1$ and $n=2$ the dynamics of the grid sites, as represented by the time evolution of $B_x(t)$ and $D(t)$, is completely deterministic and periodic. However, starting from $n=3$, the evolution becomes rather complex. The dependence of its phase-space structure on the model parameters is nonmonotonic and consists of wide domains of chaotic oscillations separated by narrow windows of regular dynamics. To obtain the correlation dimension d characterizing the chaotic regime, we used the well-known Grassberger-Procaccia formula ([12])

$$C(r)=\frac{2N_{r<R}}{N(N-1)},$$

where $N_{r<R}$ is the number of points on the Poincaré cross section separated by a distance r less than R and N is the total number of points. The results of this analysis show that the phase space of the studied subsystem has distinct fractal geometry (Fig. 2), and the current sheet model does generate a deterministic chaos on the level of local interactions.

It should be emphasized that the chaotic dynamics in the interactions of the elements of the current sheet model differs from complex behavior in a deterministic version of sandpile cellular automata. In the cellular automata driven by steady input, the dynamics can be complicated but in fact it is periodic due to the finite number of possible states [3]. The period of this dynamics strongly increases with the number of elements, and for large values of n the resulting behavior becomes unpredictable. In contrast, the complexity in the current sheet model has a low-dimensional origin and can arise at any grid site surrounded by a pair of neighbors and subjected to a flux inflow.

IV. INTEGRATED RESPONSE FUNCTION

Structurally stable critical scaling requires that the model dynamics remains near the SOC state for a finite range of the effective control parameters represented by h and ε. To check the possibility of such an effect in the current sheet model, we studied scaling features of the total susceptibility χ defined as a space and time integral of the impulse response function describing the reaction of the system to a small perturbation [8]. For a stationary perturbation, the total susceptibility can be determined as

$$\chi=\partial\rho_a(h,\varepsilon)/\partial h, \tag{3}$$

where ρ_a is the density of active grid sites averaged over space and time. As the system approaches the SOC state, the susceptibility scales with the dissipation rate ε as $\chi\sim\varepsilon^{-\gamma}$, $\gamma=1$ [8]. We consider this scaling law as the criterion for the identification of the critical region of the model. In order to obtain the expression for χ in the current sheet model, its dynamics should be analyzed in the long-term steady state. Averaging Eq. (1) over time and integrating over position for either negative or positive values of z we find that

$$S_0 2L/\pi=\langle[D(\partial B_x/\partial z)]_{z=0}\rangle_t. \tag{4}$$

Note that the left-hand side of Eq. (4) represents the input flux whereas the right-hand side describes the dissipation that takes place at the central point where the opposing fields meet and annihilate. With the chosen value of the hysteresis parameter β, the field gradient at this point always remains in the neighborhood of the critical value k and so the fluctuations of the output flux are mainly contributed by the dynamics of the diffusion coefficient. It is easy to show that at any spatial position, and in particular at $z=0$, the time average of the formal initial-value solution to Eq. (2),

$$D(z,t)=D(z,0)e^{-t/\tau}+\frac{1}{\tau}\int_0^t Q(z,s)e^{-(t-s)/\tau}ds,$$

is given by $\langle D\rangle_t=\langle Q\rangle_t$. We assume that the time average of Q at $z=0$ can be expressed in terms of the *total* spatiotemporal average of this parameter as

$$\langle Q(z=0)\rangle_t=\xi\langle Q\rangle_{z,t}, \tag{5}$$

where ξ is a numerical factor depending on the shape of the mean spatial profile of Q. The value of $\langle Q\rangle_{z,t}$, in its turn, is a function of the density ρ_a of active sites that are naturally defined by the condition $Q=D_{\max}$. Since ρ_a estimates the probability of finding a site in the active state with Q

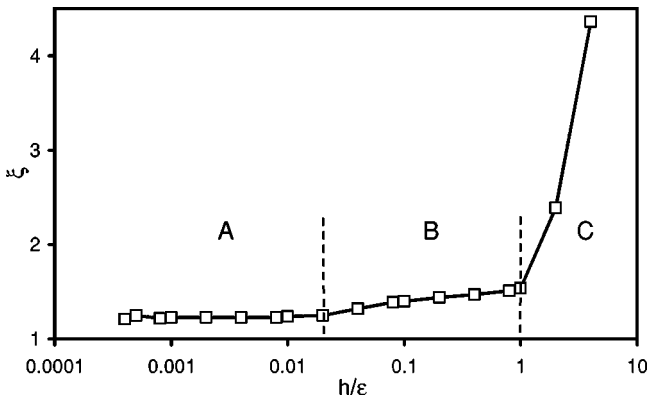

FIG. 3. Dependence of the parameter ξ entering the steady-state solution to the system (1),(2) on the reduced control parameter h/ε. Capital letters mark three main regions of system's behavior discussed in the text.

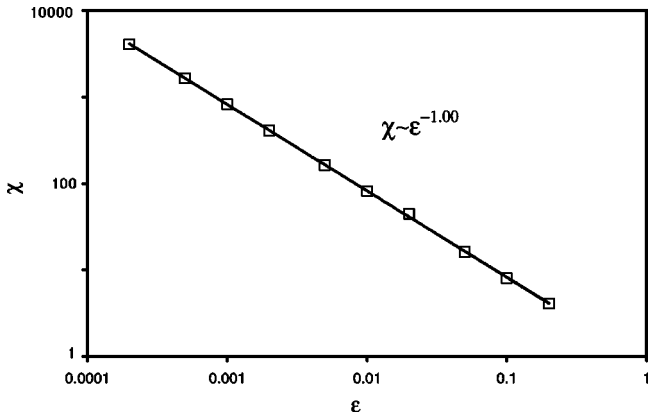

FIG. 4. Scaling of the susceptibility with the dissipation rate. The power-law fit is given by the solid line.

$=D_{\max}$, and since $D_{\min}=0$, we expect that $\langle Q\rangle_{z,t}=\rho_a D_{\max}$. Combining the above results, we obtain

$$\rho_a=\frac{(2/\pi)S_0}{\xi k D_{\max}/L}. \tag{6}$$

The numerator in this relation represents the average rate at which the source $S(z)=S_0\sin(\pi z/2L)$ adds the magnetic field to the current sheet elements and so corresponds to h. The combination $kD_{\max}/L$ in the denominator describes the average rate of annihilated flux per unit volume and is a reasonable analog for the dissipation rate ε. Hence, Eq. (6) can be rewritten in the form

$$\rho_a=h/(\xi\varepsilon),$$

$$h=(2/\pi)S_0, \quad \varepsilon=kD_{\max}/L. \tag{7}$$

It is worth noting that this steady-state solution does not imply any constraints on h and ε such as are typical for cellular automata at SOC in which the output flux is usually limited by the fixed rate at which the conserved quantity can be transported. Another important feature of Eq. (7) is that, in general, ξ is a function of both control parameters. However, if for a certain region in the control parameter space $\xi\neq\xi(h,\varepsilon)$, Eq. (7) allows us to calculate the total susceptibility (3) that scales as

$$\chi\sim 1/\varepsilon. \tag{8}$$

This formula recovers the result obtained by Vespignani and Zapperi [8] for the zero-field susceptibility in sandpile cellular automata in the limit $h\to 0$, $\varepsilon\to 0$ [8]. We have found that in the current sheet model, the region in the control parameter space over which the susceptibility exhibits power-law scaling is rather wide. Equation (7) offers a natural way to observe this effect by looking at the parameter ξ. We have numerically studied the dependence of ξ on the control parameters choosing different values of S_0 and k so that the driving and the dissipation rates varied in the ranges $2\times10^{-6}\ldots 2\times10^{-1}$ and $2\times10^{-4}\ldots 2\times10^{-1}$, respectively. The preliminary analysis has shown that it is not h and ε taken separately but the reduced variable h/ε that actually controls the state of the system. Any pairs of h and ε that have the same ratio lead to the same ξ. So, in order to find a dynamical regime characterized by constant ξ, it was enough to study this parameter as a function of h/ε.

We have found that the dependence $\xi(h/\varepsilon)$ consists of three distinct regions (Fig. 3). For $h/\varepsilon<2\times10^{-2}$ (region A), ξ as a function of the reduced control parameter is practically constant, and so we expect that $\partial\xi/\partial h=\partial\xi/\partial\varepsilon=0$ and $\chi\sim 1/\varepsilon$ in accordance with Eq. (8). Based on the finite range of the driving and dissipation rates that produces power-law divergence of the integrated response function, we identify this regime as structurally stable critical scaling. To confirm the critical behavior of χ in the region A of Fig. 3, we constructed a series of plots showing active site density versus driving rate for different dissipation rates. In each plot we selected a linear segment corresponding to $h/\varepsilon<2\times10^{-2}$ and found its slope to estimate χ at the present ε. The results show that in this region, the total susceptibility obeys a power-law relation (8) over at least three decades of the dissipation rate with a remarkably high accuracy (Fig. 4).

For h/ε values higher than 2×10^{-2} (region B in Fig. 3), ξ starts to respond to changes in the reduced control parameter; however, since the response is still very weak, this behavior can be considered almost critical. Starting from $h/\varepsilon\approx 1$ (region C), to retain the stationary flux balance the parameter ξ increases sharply, and the system loses its critical properties.

Our previous studies of the model [13] suggest that the point of the transition between the regions A and B corresponds to the disappearance of the global loading-unloading cycle. At this point, the loading periods become so short that the systemwide discharge events start merging. This observation gives some hint about the origin of the robust critical dynamics in region A. As long as the loading-unloading cycle exists, the model can adjust to changes in the control parameters by varying the loading interval. This mechanism allows the system to maintain a stationary state without changing the scaling features of the turbulent unloading dynamics associated with the SOC avalanches. This is in contrast to other avalanche models, which normally miss the global loading-unloading cycle and can only adjust to changes in h or ε by reorganizing the avalanche dynamics.

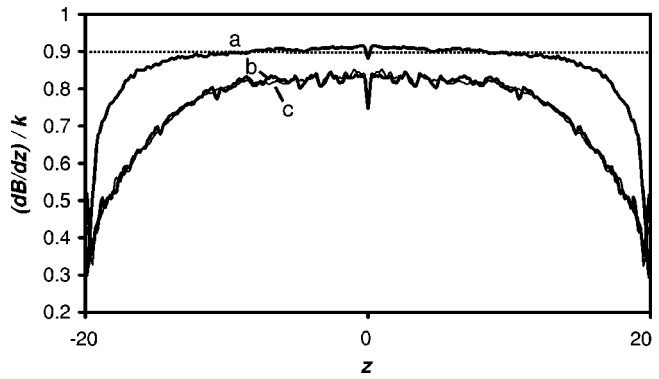

FIG. 5. Three examples of spatial profiles of the normalized magnetic field gradient $(\partial B_x/\partial z)/k$: (a) $h=10^{-3}$, $\varepsilon=10^{-2}$, $h/\varepsilon=10^{-1}$; (b) $h=10^{-6}$, $\varepsilon=5\times10^{-4}$, $h/\varepsilon=2\times10^{-3}$; (c) $h=2\times10^{-5}$, $\varepsilon=10^{-2}$, $h/\varepsilon=2\times10^{-3}$. Each profile was averaged over several global unloading events involving 5000 to 10 000 individual avalanches. The dotted horizontal line corresponds to $\partial B_x/\partial z=\beta k$.

To better understand the nature of the observed robust critical scaling, it is instructive to return to the definition of ξ. According to Eq. (5), the absence of the dependence of ξ on the control parameters implies a globally stable spatial configuration of the magnetic field making it possible to express the quantity $\langle Q(z=0)\rangle_t$ as a constant fraction of the spatiotemporal average $\langle Q\rangle_{z,t}$. The numerical investigation of field profiles averaged over several global unloading events has confirmed this effect (Fig. 5). It has been found that the shape of the field gradient looks almost identical for quite different h and ε values, provided h/ε belongs to the region A in Fig. 3, and changes dramatically as h/ε goes outside the critical region.

V. CONCLUSION

We have shown that the current sheet model displays a hierarchy of turbulent effects. On the scale of local interactions, its dynamics is affected by a nonlinear deterministic chaos that is the source of randomness in the model. The local chaos appears to be in an interesting symbiosis with the scale-free avalanche dynamics that transmits the dynamical uncertainty over a wide range of scales making the behavior of the whole system practically unpredictable.

On the global scale, the continuum current sheet model exhibits structurally stable critical scaling consistent with a finite range of the reduced control parameter h/ε and at nonzero values of the driving rate. In this state, the system shows a power-law divergence of the integrated response function over a broad range of the dissipation rate. The robust features of the model dynamics are closely connected to the global loading-unloading cycle that allows a long-term steady state without affecting the intrinsic avalanche dynamics. We have also found that the observed critical behavior involves a remarkably stable time-averaged spatial distribution of the magnetic field, which tends to self-organize into a unique stationary configuration.

These findings lead us to a more general picture for the structure of the attracting critical state. We suggest that an observation of scaling effects associated with SOC does not necessarily require fine-tuning these parameters to zero. In continuum avalanche systems with a global loading-unloading cycle, a rather rough tuning might be sufficient to obtain near-critical behavior displaying characteristic features of SOC state. Such tuning conditions may be met in a large variety of open systems with extended degrees of freedom, space physics systems included.

ACKNOWLEDGMENTS

We thank J. Valdivia, N. Watkins, and A. Vespignani for useful discussions. The work of V.M.U. was supported by the National Research Council at NASA / Goddard Space Flight Center.

[1] P. Bak, C. Tang, and K. Wiesenfeld, Phys. Rev. Lett. **59**, 381 (1987).
[2] P. Bak, C. Tang, and K. Wiesenfeld, Phys. Rev. A **38**, 364 (1988).
[3] K. Wiesenfeld, J. Theiler, and B. McNamara, Phys. Rev. Lett. **65**, 949 (1990).
[4] A. Diaz-Guilera, Europhys. Lett. **26**, 177 (1994).
[5] L. Gil and D. Sornette, Phys. Rev. Lett. **76**, 3991 (1996).
[6] T. Tsuchiya and M. Katori, Phys. Rev. E **61**, 1183 (2000).
[7] O. Kinouchi and C. Prado, Phys. Rev. E **59**, 4964 (1999).
[8] A. Vespignani and S. Zapperi, Phys. Rev. E **57**, 6345 (1998).
[9] E. Lu, Phys. Rev. Lett. **74**, 2511 (1995).
[10] A.J. Klimas, J.A. Valdivia, D. Vassiliadis, D.N. Baker, M. Hesse, and J. Takalo, J. Geophys. Res., [Space Phys.] **105**, 18 765 (2000).
[11] V. Uritsky, A.J. Klimas, J.A. Valdivia, D. Vassiliadis, and D.N. Baker, J. Atmos. Sol.-Terr. Phys. **63**, 1425 (2001).
[12] P. Grassberger and I. Procaccia, Physica D **9**, 189 (1983).
[13] A. Klimas, V. Uritsky, J. Valdivia, and D. Vassiliadis, in *Proceedings of the 5th International Conference on Substorms*, edited by A. Wilson (ESA, St. Petersburg, Russia, 2000), p. 165.